

Chapter 9

Soft Crystal Chemiluminescence Systems Using Organic Peroxides



Takashi Hirano  and Chihiro Matsushashi 

Abstract Chemiluminescence (CL) is a phenomenon in which a chemical reaction produces an excited-state product that emits light. Taking advantage of this property, several analytical methods to study the CL reactions by photon detection have been developed in the literature. By applying this methodology to molecular crystals, soft crystal CL systems have been constructed to analyze the intracrystalline reactions of chemiluminescent compounds. In this chapter, the fundamental concept and applications of CL are presented. Using the example of the CL reactions involving organic peroxides, important characteristics of CL such as chemiexcitation, quantum yield and emission wavelengths are discussed. Furthermore, CL in solid state and in molecular crystals are described. Finally, the application of organic peroxides as a soft crystal CL system and the characteristics of their intracrystalline reactions such as crystal structure-dependencies, reaction kinetics and inductions of phase transitions are elucidated. This chapter concludes with a brief outlook towards the future of soft crystal CL systems.

Keywords Chemiluminescence · Organic peroxide · 1,2-Dioxetane · Crystalline-state reaction · Real-time analysis

9.1 Introduction: Research Significance of Soft Crystal Chemiluminescence Systems

Chemiluminescence (CL) is a phenomenon in which light is emitted during a chemical reaction that yields an electronically excited product [1–3]. Soft crystal CL systems are a group of crystalline materials that demonstrate CL during chemical reactions in crystals with soft properties. A “soft property of a crystal” means that the crystal has a property to undergo its facile structural transformation and phase transition in response to weak but specific stimuli. Basic and applied research studies

T. Hirano (✉) · C. Matsushashi

Department of Fundamental Science and Engineering, Graduate School of Information Science and Engineering, The University of Electro-Communications, Chofu, Tokyo 182-8585, Japan
e-mail: thirano@uec.ac.jp

© The Author(s) 2023

M. Kato and K. Ishii (eds.), *Soft Crystals*, The Materials Research Society Series,
https://doi.org/10.1007/978-981-99-0260-6_9

155

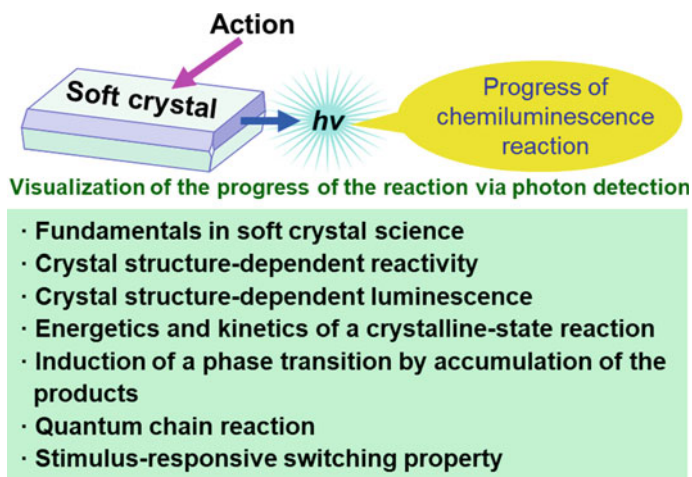


Fig. 9.1 Application of chemiluminescence in soft crystal science

on CL have been conducted as CL is a useful analytical technique when used along with photon detection, especially in the crystalline state chemistry (Fig. 9.1). For instance, if CL is induced by a mechanical force, as seen in the mechanochemistry of polymers described below, the applied stress can be optically detected. In this way, the chemical reaction in the crystal can be visualized.

A crystalline-state reaction has the advantage of yielding a selective product that reflects the crystal structure of the reactant. In fact, crystalline-state photochemical reactions of organic compounds and photochemical and thermal polymerizations of alkynes in crystals have been studied for a long time [4–6], which provided important reaction modes. Recently, mechanochemical methods, which involve mixing crystals mechanically, have been developed for organic synthesis [7, 8], to pioneer environmentally friendly reactions. In the field of pharmaceutical sciences, drugs are often dosed in the crystalline state; therefore, it is necessary to understand the reactivity of these drugs, especially the kinetics, in the crystalline state to understand their stability [9, 10]. Because of all of these current and potential applications, studying the basic theory of the chemical reactions that occur in crystals is important. In particular, the “soft property of crystals”, i.e., a property of the crystal that changes the molecular and crystal structures during chemical reactions, is an important research topic (Fig. 9.1) [11]. However, several unresolved problems must be addressed in crystalline-state chemical reactions which require an understanding of the relationships between crystal structures and reactivities, the energetics and kinetics of reactions, the mechanism of tuning the luminescence properties within crystals, and the mechanism of “action” responsiveness based on the fundamental theories. Soft crystal CL systems are a valuable tool to address these problems and to visualize and track the progress of intracrystalline reaction. In this context, in recent years, efforts to elucidate the reaction mechanisms of crystalline-state CL reactions and to

construct a fundamental theory of intracrystalline reactions have been underway. In this chapter, first, we will discuss the fundamentals and general usefulness of the CL reactions of organic peroxides, followed by the features of peroxide CL in the solid state and condensed state and those in molecular crystals. In particular, characteristics of intracrystalline reactions that have recently been revealed by soft crystal CL systems will be described, followed by a future perspective.

9.2 Characteristics of the Chemiluminescence Reactions of Organic Peroxides

9.2.1 Real-Time Analysis by Photon Detection

As described above, CL is luminescence caused by a chemical reaction, which includes bioluminescence (BL) seen in a firefly or a sea firefly. In analytical chemistry, we exert an “action” on a “sample” and detect its “response” to obtain the necessary information, such as the concentration, mass, or physical properties, on the target material in the sample. Because a CL reaction generates photons, we can recognize that “a chemical reaction has occurred” by photon detection (Fig. 9.2). Therefore, CL is widely used as an analytical method because the “response” to the “action” of the CL during the reaction can be detected optically [12]. It is well known that the CL of luminol is used for bloodstain detection and the firefly BL reaction is used for ATP detection; these reactions are based on the fact that the analyte is an essential factor in the reaction progression. For instance, hemoglobin in the blood catalyzes the acceleration of the CL reaction of luminol, and ATP is the reagent responsible for the activation (adenylation) of firefly luciferin (Fig. 9.3). Because the presence or absence of an analyte and its abundance can be confirmed by photon detection, information on the production, consumption, and transfer of the analyte can be traced by relying on the luminescence.

A representative example of this is the firefly BL reaction. Firefly BL is based on the luciferin-luciferase (L-L) reaction involving the substrate, firefly luciferin and the enzyme, luciferase; this reaction requires ATP and oxygen to react with luciferin and Mg^{2+} to activate the enzyme [13, 14]. All the above substrates and reagents are essential to produce photons in the L-L reaction; hence, all of them can be marked as analytes whose presence can be confirmed by luminescence. Luciferase is created through gene expression in a cell and is lost due to degradation. Since ATP, oxygen, and Mg^{2+} are normally present in the cell, gene expression and migration of luciferase in the cell can be tracked by photon detection by injecting luciferin into the cell (Fig. 9.2e). The same analysis can be performed in vivo in a mammal, such as a mouse, enabling us to “watch” (analyze) the reaction in a living organism in real time via BL imaging [15–17]. This ability of “real-time analysis” by photon detection is the most attractive aspect of CL [18, 19].

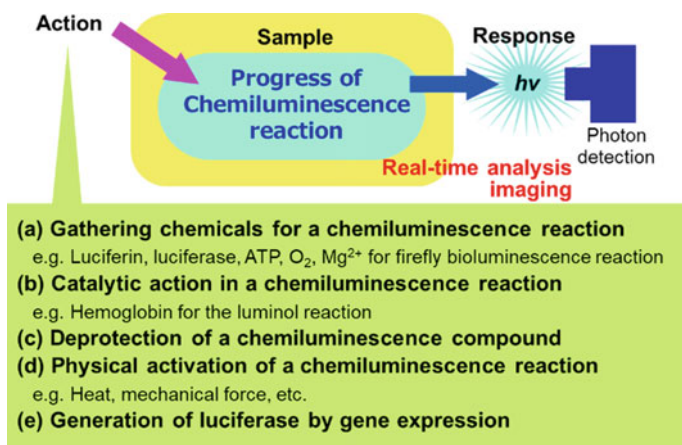


Fig. 9.2 Chemical analyses of chemiluminescence reactions

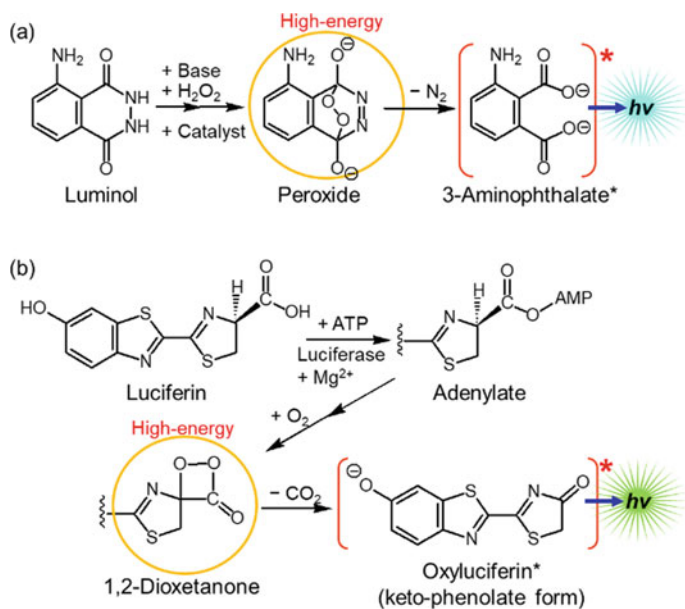


Fig. 9.3 **a** Chemiluminescence reaction of luminol and **b** bioluminescence reaction of firefly luciferin

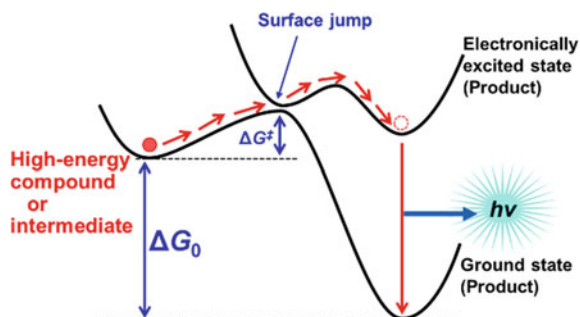
9.2.2 Chemiexcitation, Quantum Yield and Emission-Wavelength Regulation

For a chemical reaction to produce photons, in most cases, the reaction must be exothermic, in which the energy emitted must be equivalent to that required for the production of photons. The CL reaction of luminol proceeds with O_2 or hydrogen peroxide under basic conditions via a cyclic peroxide intermediate, whose thermal decomposition gives the excited-state product, which emits light (Fig. 9.3a). In the firefly BL reaction, the adenylated form of luciferin gives a cyclic peroxide intermediate via oxygen addition and its thermal decomposition gives the excited-state product (Fig. 9.3b). Many chemiluminescent compounds involve such peroxide intermediates in their reactions. Thus, the essence of CL lies in the fact that a peroxide intermediate acts as a high-energy compound, which yields the essential emissive excited-state product by thermal decomposition (Fig. 9.4). This process is called “chemiexcitation”. For chemiexcitation to occur, the process must be an exothermic reaction and the energy difference between the transition state of the high-energy compound and the ground-state products must be sufficient to emit light. The peroxide intermediates described above satisfy the chemiexcitation conditions.

Notably, the peroxide intermediate in the firefly reaction is a 1,2-dioxetanone, which is a derivative of the 1,2-dioxetane and a historically key structure involved in the BL reactions [2, 3]. 1,2-Dioxetanes have a strained four-membered ring structure with an O–O bond, which easily undergoes a ring-opening reaction to yield two carbonyl products by the cleavage of O–O and C–C bonds. Among the 1,2-dioxetane derivatives, 3,3,4,4-tetramethyl-1,2-dioxetane (TMD) has been studied the most, as a representative derivative, to develop the energy diagram for the thermal decomposition reaction to yield the excited singlet (S_1) or excited triplet (T_1) states of the product acetone (Fig. 9.5) [20, 21]. The activation energies of the thermolytic reactions and the efficiencies for generating excited-state products of 1,2-dioxetane derivatives have been widely studied [22, 23].

The efficiency with which the excited-state product is generated by the thermal decomposition of a 1,2-dioxetane derivative is termed as chemiexcitation efficiency, which is an important CL property. For instance, the L-L reaction using firefly

Fig. 9.4 Chemiexcitation process of a high-energy compound or intermediate



is electron-donating (D) and the 1,2-dioxetanone is electron-accepting (A), which leads to an intramolecular electron transfer and subsequent decomposition of 1,2-dioxetanone generates the oxyluciferin radical and the CO_2 radical anion. When the CO_2 radical anion transfers an electron to the oxyluciferin radical, oxyluciferin in the S_1 state (phenolate anion) will be generated with high efficiency [27]. This mechanism is called the CIEEL (chemically initiated electron exchange luminescence) mechanism.

Subsequent theoretical calculations lead to a modification of the CIEEL mechanism to the CTIL (charge transfer induced luminescence) mechanism, in which the reaction proceeds by intramolecular charge transfer instead of electron transfer [28]. In the CTIL mechanism, unlike the homolytic bond cleavage mechanism described above, the chemiexcitation proceeds through the transition state in the S_1 state which has a high charge-transfer ability and a reduced biradical character. The CTIL mechanism of the 1,2-dioxetanone intermediate of the firefly BL reaction proceeds so rapidly that the intermediate has not been directly observed to date; however, its existence has been confirmed by isotope experiments. In general, CL reactions via the CTIL mechanism proceed rapidly. On the other hand, stable 1,2-dioxetane derivatives have been found, including TMD, whose thermolytic reactions proceed by the homolytic bond cleavage mechanism. Three groups of compounds with the adamantane moiety are representative examples of stable 1,2-dioxetanes (Fig. 9.6: Adox, Ad-OSi, and Ad-Acr) [29–31]. Among them, adamantylideneadamantane 1,2-dioxetane (Adox) has the highest thermal stability [3, 32]. The stability of these derivatives is attributed to the inhibition of the elongation of the O–O bond to give a trapezoidal shape to the 1,2-dioxetane ring before the homolytic bond cleavage. This deformation results in a spatial proximity between the substituents attached to C3 and C4 of the 1,2-dioxetane ring. In the case of the thermal decomposition of Adox, the two adamantane moieties must be brought spatially closer, which requires a relatively high activation energy. Then, Adox has a thermal stability. Other 1,2-dioxetanes with the adamantane moiety also have a thermal stability in the similar manner to Adox. Among the three compounds Adox, Ad-OSi, and Ad-Acr, Ad-OSi demonstrates a reactivity change by silyl-deprotection [30]. Ad-OSi is easily converted to unstable Ad-O^- by a reagent for silyl-deprotection. The 1,2-dioxetane ring in Ad-O^- is connected to the electron-donating moiety and activates the CTIL mechanism, leading to a fast reaction rate and generation of the S_1 -state product with high efficiency. Thus, the stability of a 1,2-dioxetane derivative can be manipulated by deprotection. Moreover, this technique is useful for analyzing a deprotection reagent. For example, by replacing the silyl group of Ad-OSi with the acetyl group, the enzymatic action of an esterase for ester hydrolysis can be analyzed by photon detection (Fig. 9.2c) [33].

As the important characteristics of CL reactions, the regulation of the efficiency and reaction rate of the chemiexcitation have been discussed. The chemiexcitation efficiency is an important component of the CL quantum yield (Φ_{CL}). That is, for a CL reaction that emits photons from the S_1 state products, the Φ_{CL} value is described as follows:

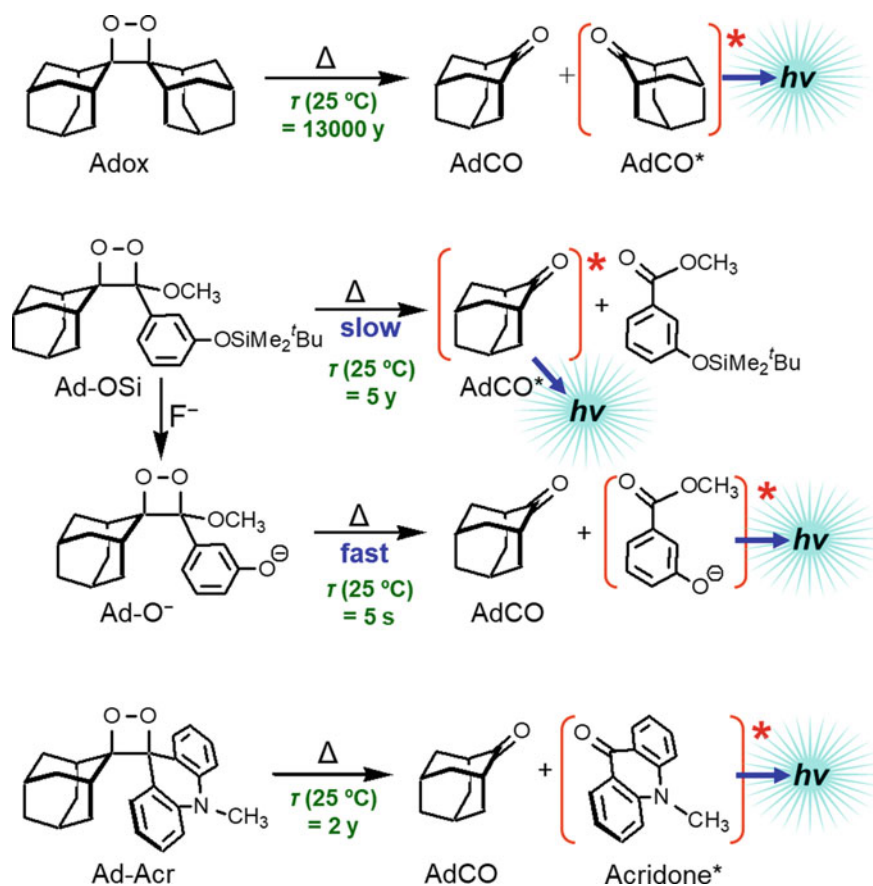


Fig. 9.6 Chemiluminescence reactions of stable 1,2-dioxetanes

$$\Phi_{CL} = \Phi_R \times \Phi_S \times \Phi_F \quad (9.1)$$

where Φ_R is the reaction efficiency to afford the main products in the ground and excited states, Φ_S is the chemiexcitation efficiency to yield the product in the S_1 state by decomposition of the high-energy intermediate, and Φ_F is the fluorescence emission efficiency of the product in the S_1 state. Eq. (9.1) is applicable to the analysis of a Φ_{BL} value. In the case of the thermolytic reaction of a 1,2-dioxetane, two carbonyl products are obtained quantitatively, indicating $\Phi_R = 1$. Thus, the equation becomes

$$\Phi_{CL} = \Phi_S \times \Phi_F \quad (9.2)$$

Another important characteristic of the CL reactions is the emission wavelength, which is determined by the nature of the excited-state product of the reaction. Most of the CL reactions including BL reactions produce light from the S_1 -state products.

For instance, in the CL reaction of luminol, blue emission occurs from the S_1 state of 3-aminophthalate (Fig. 9.3a). In the firefly BL reaction, the phenolate anion of oxyluciferin, which is in the S_1 excited state, emits green to red light (Fig. 9.3b) [34]. The visible light emission wavelength (i.e., color) can be varied by adjusting the stability of the S_1 state of oxyluciferin in the active site of luciferase. The thermolytic reaction of TMD shows violet emission from the S_1 state of acetone, while its Φ_{CL} value is low, owing to the low Φ_S value to generate the S_1 -state acetone and the low Φ_F value of acetone Eq. (9.2).

To analyze CL, a desired emission wavelength must be obtained. To achieve this, one method is to adjust the π -electronic system of the excited state product. In the case of the CL reaction of a 1,2-dioxetane derivative, the fluorescence emission wavelength of either of the two carbonyl products can be adjusted. The thermolytic reaction of the stable 1,2-dioxetane derivative Ad-Acr, for instance, yields 2-adamantanone (AdCO) and acridone as the products. Because acridone has a wider π -electronic system than AdCO, the S_1 state of acridone is preferentially generated by chemiexcitation and shows blue-light emission (Fig. 9.6) [31].

Chemiluminescence resonance energy transfer (CRET) is another method to achieve a desired emission wavelength. When a fluorophore is linked to a chemiluminescent moiety in a non-conjugated manner, intramolecular Förster-type resonance energy transfer can take place from the S_1 -state product of the chemiluminescent moiety to the fluorophore moiety [35], thus achieving emission from the fluorophore moiety. This mechanism is named CRET, similar to fluorescence resonance energy transfer (FRET), which is the resonance energy transfer between two fluorescent dyes. If the product generated from the chemiluminescent moiety has a low Φ_F value, CRET can be applied to improve Φ_{CL} . When the intermolecular distance between the chemiluminescent and fluorophore moieties is shortened, CRET aids in modulating the emission wavelength. Several living organisms, such as the jellyfish *Aequorea*, have also utilized CRET in their BL reactions [36]. This jellyfish has a photoprotein, aequorin, which has the chemiluminescent compound in the apoprotein, and a green fluorescent protein (GFP), which has a fluorophore within a β -barrel structure. The S_1 -state product generated within the apoprotein of aequorin usually emits blue light. However, aequorin and GFP, which are in close proximity to each other, experience energy transfer from the S_1 -state product of aequorin to GFP, resulting in the emission of green luminescence. This mechanism is called bioluminescence resonance energy transfer (BRET), which is a BL version of CRET. On a related note, aequorin has a Ca^{2+} -chelating site (EF hand), and this Ca^{2+} -binding triggers the BL reaction in aequorin. Therefore, aequorin has been used as a BL indicator for Ca^{2+} (Fig. 9.2a).

In this section, we reviewed the chief characteristics and reaction mechanisms of CL, including BL. For the explanations, we described the thermolytic reactions of 1,2-dioxetanes, which are the representative high-energy compounds. The bicyclic peroxide intermediate derived from luminol was also an example of a high-energy compound for chemiexcitation (Fig. 9.3a). As other peroxides for CL reactions, two examples will be introduced here. One is diphenoyl peroxide (Fig. 9.7), which shows CL when in combination with an electron-donating aromatic compound. This

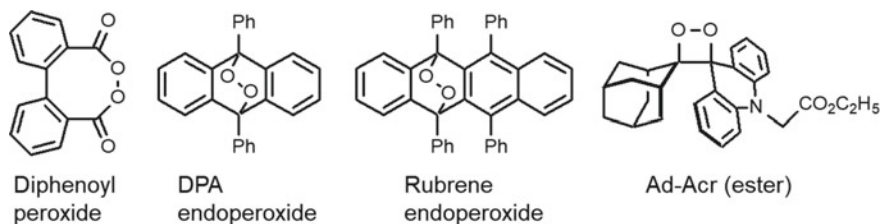


Fig. 9.7 Organic peroxides capable of chemiluminescence

peroxide was used to elucidate the CIEEL mechanism [37]. Another is an endoperoxide of an aromatic hydrocarbon. Interestingly, endothermic thermolytic reactions of endoperoxides of naphthalenes and anthracenes show CL [38]. For example, the endoperoxide of 9,10-diphenylanthracene (DPA) (Fig. 9.7) thermally decomposes to give DPA and a singlet oxygen [39]. The singlet oxygen is converted to the triplet state accompanied by near-infrared light emission (1270 nm), demonstrating that it is a CL reaction. Although this reaction is endothermic and not exothermic, CL is achieved because the singlet oxygen is generated according to the spin conservation law. Thus, the CL reactions of the endoperoxides of aromatic hydrocarbons have different chemiexcitation character from those of other peroxides including 1,2-dioxetanes.

9.3 Chemiluminescence in the Solid State and Condensed State

CL is a useful analytical tool for photon detection; therefore, studies have focused mainly on its application in solution. Although CL in the solid state has been known for a long time, there have only been a few systematic studies. In 1926, Moureau et al. reported that heated crystals of rubrene endoperoxide (Fig. 9.7) emitted red light; the reaction mechanism remains unresolved to date [40, 41]. Crystals of Adox were also known to glow during thermal analysis [42]. In addition, studies of CL were conducted by heating the solid samples to analyze the subsequent reaction and to access the condensed state. A condensed state including the crystalline state is a state of high concentration, in which intermolecular interactions and energy transfer are expected to be favored.

In a condensed state, the photoreactivity of 1,2-dioxetane is related to the CL reaction, to make a quantum chain reaction [43]. In the photoreaction reaction of 1,2-dioxetane, the carbonyl products are formed in the S_1 and T_1 states similar to the thermolytic reaction. When the photoreaction of the 1,2-dioxetane derivative is conducted in a condensed state, the excited-state product enables energy transfer to the unreacted 1,2-dioxetane derivative, resulting in its decomposition. This process triggers a quantum chain reaction with a high quantum yield. For example, the quantum chain

photoreaction of TMD in a solution has a quantum yield that exceeds 200 [44]. A similar reaction was reported using solid-state Adox where a condensed state was obtained by concentrating a mixed solution of Adox and a lanthanide ion complex such as $\text{Eu}(\text{fod})_3$ [45]. A lanthanide ion complex catalyzes the thermal decomposition of 1,2-dioxetane, in addition to acting as an energy acceptor for light emission. Therefore, this combination of Adox and a lanthanide ion complex in the condensed state demonstrates a successful synergistic CL with the quantum chain reaction. Another example of CL in condensed state was demonstrated with a stable 1,2-dioxetane derivative with the acridane moiety, Ad-Acr(ester) (Fig. 9.7) [46]. Ad-Acr(ester) derivatives, which are used for the surface modification of silica nanoparticles, were employed to design an analytical technique for the CL analysis of a biomolecule in a condensed state on the surface of nanoparticles.

Furthermore, the mechanochemical applications of CL have recently been reported in the field of polymer chemistry [47, 48]. Adox, a stable chemiluminescent moiety, was introduced into polymers to synthesize various chemically modified derivatives. The mechanochemical CL properties of these modified polymers were then investigated. When the two ends of a polymer film were pulled in opposite directions, the applied stress induces bond cleavage of the 1,2-dioxetane rings of the Adox moieties, resulting in CL. The bond cleavage can be observed by photon detection in real time (Fig. 9.2d). This idea was realized by a rubber-like network polymer with an Adox structure inserted into poly(methyl acrylate) [49]. When the polymer film was cleaved mechanically by applying sufficient stress until the stretching force exceeded a certain threshold, CL was observed. By using this methodology, the molecular mechanism of the damage in the polymer chains depending on the magnitude of applied stress has been elucidated. Similar experiments on the mechanochemical damages were conducted on various polymers such as polyamides and polyesters [47, 48]. Moreover, the use of fluorescent dyes in Adox-bearing polymers to effectively modulate CL via CRET has also been reported [47, 48].

9.4 Chemiluminescence in Molecular Crystals

9.4.1 Mechanistic Studies of Chemiluminescence Reactions in Crystals

Studies on the reaction mechanisms of the crystalline-state CL have been reported recently [50, 51]. A single-step reaction such as the thermolytic reaction of 1,2-dioxetane can be applied to the study of crystalline-state CL; therefore, CL reactions of organic peroxides have been investigated using their molecular crystals.

The first studies to correlate the crystal structures with luminescence properties in crystals were the CL reactions of the stable 1,2-dioxetane derivative Ad-OH and the bicyclic dioxetane derivatives Dx-AOH, Dx-BOH and Dx-AOCH₃ (Fig. 9.8a)

[50]. The bicyclic dioxetane structure has been precisely designed by taking advantage of the stabilizing factors in the molecular structure of Ad-OH as explained in Sect. 9.2.2 [52]. The stability of these compounds is advantageous for preparing crystal samples with a purity to study. In Dx-AOCH₃, the phenolic hydroxy group is protected by the methyl group. Ad-OH, Dx-AOH and Dx-BOH yielded the corresponding phenolate anions by the action of a base in solution. The anions promptly decomposed to exhibit CL via the CTIL mechanism. The phenolate anions of the 3-hydroxybenzoate moieties (the CL reaction of Ad-O⁻ in Fig. 9.6), which are the light-emitters, showed emission with the maxima at 460–500 nm. Crystal samples of the four dioxetanes were heated at temperatures below their melting points to initiate their CL reactions. While the methoxy derivative Dx-AOCH₃ showed only weak CL, the CL emission spectra for the hydroxy derivatives were measurable. The CL of Ad-OH and Dx-AOH was emitted from the excited states of the phenolate anions of their 3-hydroxybenzoate moieties, whereas that of Dx-BOH was emitted from the excited state of the neutral 3-hydroxybenzoate moiety. The crystal structures of Dx-AOH and Dx-BOH indicated that the hydroxy groups of the 3-hydroxyphenyl moieties form hydrogen bonds with the oxygen atoms of the 1,2-dioxetane rings (Fig. 9.8b). When the crystal samples were heated, the oxygen atom of the 1,2-dioxetane ring assisted the deprotonation of the phenolic hydroxy group via hydrogen bonding, which promoted the decomposition of the 1,2-dioxetane ring via the CTIL mechanism. Because the donor–acceptor distance in the hydrogen bonding in Dx-AOH is relatively short (1.93 Å), the phenolate anion of the 3-hydroxybenzoate moiety is effectively generated as the excited-state product for light emission (Fig. 9.8b). In the case of Dx-BOH, the hydrogen bonding donor–acceptor distance is relatively long (2.02 Å); therefore, the deprotonation does not occur and the excited state of the neutral 3-hydroxybenzoate moiety is responsible for light emission (Fig. 9.8b). These results confirmed that the crystal structures determine the CL behavior. Moreover, the CL reaction of the crystalline-state Dx-AOH which is heated to 100 °C demonstrated first-order reaction kinetics. This relationship between the reaction kinetics and the crystallinity is a significant issue to consider because a reaction in the crystalline state destroys the crystal structure.

Crystalline-state CL reactions of lophine hydroperoxide (LHP) were also studied by photon detection [51]. Lophine is the first artificially synthesized CL compound, which reacts with O₂ under basic conditions to demonstrate CL via the hydroperoxide anion of LHP [53]. A plausible reaction mechanism is the formation of a 1,2-dioxetane intermediate from the LHP anion, which undergoes chemiexcitation upon thermal decomposition to yield the S₁-state benzoylamidine anion for light emission (Fig. 9.9) [54]. LHP was prepared by the ene reaction of lophine with a singlet oxygen. In solution, the CL reaction of LHP can be initiated by the action of a base via the abovementioned pathway. Recrystallization of LHP yielded cm-size crystals, which were used for crystalline-state CL reactions. The thermolytic reaction of crystalline LHP produced the major products lophine and O₂ along with the minor products benzoylamidine and an unidentified product in less than 5% yield. During this reaction, the bubbling of oxygen from the heated crystals was observed. The CL emission maximum observed at 530 nm suggests the emission of phosphorescence

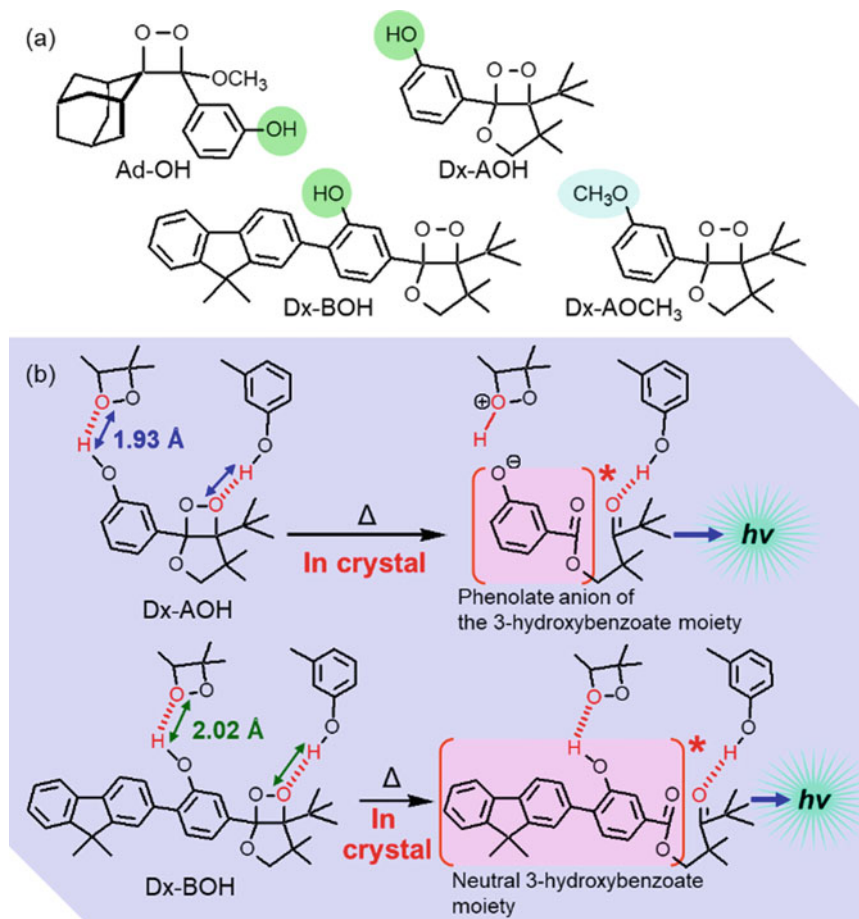


Fig. 9.8 **a** 1,2-Dioxetane derivatives for crystalline-state chemiluminescence and **b** CL reactions of crystalline-state Dx-AOH and Dx-BOH

from the T_1 state of the lophine anion (Fig. 9.9). Furthermore, the study reported the CL emission spectra of the heated crystal samples of Adox, rubrene endoperoxide, and benzoyl peroxide. This study by Schramm et al., like the study reported by Watanabe et al. on the crystalline-state 1,2-dioxetane derivatives, also raises an important question regarding the dynamic relationship between the reaction progress and the structural change in crystals.

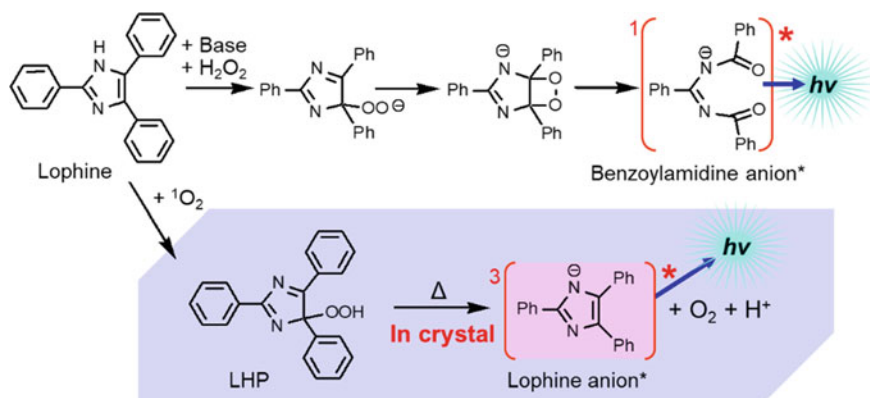


Fig. 9.9 Chemiluminescence reactions of lophine and lophine hydroperoxide (LHP)

9.4.2 Exploring the Science of Intracrystalline Reactions with Soft Crystal Chemiluminescence Systems

Mechanistic studies on the progress of crystalline-state reactions and the corresponding dynamic changes in the crystal structures owing to the accumulation of reaction products were conducted based on the concept of soft crystal science [11]. That is, a “soft property of a crystal” is expected to allow the structural change and phase transition of the crystal in response to the accumulation of reaction products. In this section, the relationships between the crystal structures, the luminescence properties and reactivity were elucidated with soft crystal CL systems.

Matsuhashi et al. adopted Adox derivatives as the CL substrates for their soft crystal CL system to study intracrystalline reactions. Adox derivatives were synthesized by linking fluorophore moieties to tune the CL properties of the crystals (Fig. 9.10) [55, 56]. Adox derivative **1** with a fluorophore side chain (FL1: *N*-(4-trifluoromethylphenyl)phthalimide) has two stereoisomers (*syn*-**1** and *anti*-**1**). In the case of di-substituted derivative **2**, there are three stereoisomers (*cis-syn*-**2**, *cis-anti*-**2**, and *trans*-**2**) and 5-(4-methoxyphenyl)-*N*-(4-trifluoromethylphenyl)phthalimide was used as a fluorophore moiety FL2. Utilization of the stereoisomers is advantageous in the evaluation of a reactivity change caused by the difference in the crystal structures, because the isomers have similar reactivity in solution. In addition, the fluorophore moieties in **1** and **2** will accept energy from the excited state of a neighboring AdCO moiety via the CRET mechanism as previously explained in Sect. 9.2.2. Because AdCO has a low Φ_F of approximately 0.001 in solution, the Φ_{CL} value was expected to improve after the energy transfer. Furthermore, the fluorophore moiety was expected to tune emission wavelength, control crystallinity and form an excited dimer or complex. For the design of di-substituted derivative **2**, the fluorophore FL2 was adopted in place of FL1, because FL2 showed stronger fluorescence than FL1.

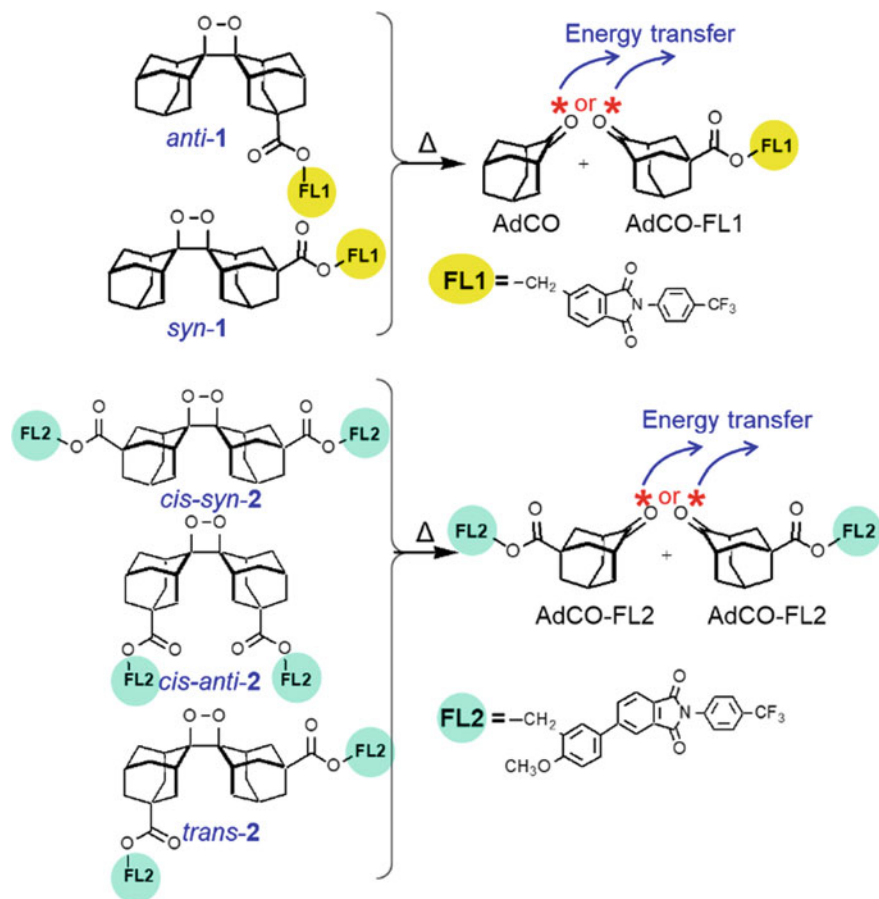


Fig. 9.10 Chemiluminescence reactions of the isomers of fluorophore-linked Adox derivatives **1** and **2**

Mono-substituted derivatives *syn-1* and *anti-1* showed clear differences in crystal structures, CL emission properties and reactivities [55]. When the crystal samples of *syn-1*, *anti-1*, and Adox were heated to 160 °C, they all showed CL with the emission maxima of 465 nm, 440 nm, and 430 nm, respectively. Interestingly, the CL of *syn-1* is caused by distinct energy transfer. Upon heating, the CL intensity for *syn-1* was stronger than that for Adox, while the CL intensity for *anti-1* was weaker than that for Adox. This is because the CL intensity depends on both the CL quantum yield Φ_{CL} and the reaction rate ($-d[R]/dt$, where $[R]$ is the reactant concentration). Because the reaction rate in crystals for *syn-1* was faster than that for *anti-1*, *syn-1* had the higher CL intensity. Morphological observations of the heated crystals also showed a characteristic difference. The crystals of *syn-1* started melting at approximately 3 min after the heating had begun, whereas *anti-1* maintained its crystalline state for approximately 15 min after the heating had begun. It is evident

that the differences in the luminescence properties, reaction rates, and the abilities to maintain the crystalline state upon heating reflect the differences in the crystal structures. In fact, *syn-1* has a crystal structure in which Adox and FL1 moieties are stacked alternately along the *b*-axis, whereas *anti-1* has a crystal structure in which Adox and FL1 moieties are in separate aggregated layers (Fig. 9.11). The thermolytic reactions of *syn-1* and *anti-1* generated the excited states of either AdCO or the AdCO moiety in AdCO-FL1 (Fig. 9.10). In the crystal of *syn-1*, the energy transfer from the excited state of either AdCO or the AdCO moiety to the FL1 moiety in a neighboring molecule is efficient because of the alternated layer structure of the crystal in which both the species are in close proximity to each other. On the other hand, in the crystal of *anti-1*, the excited-state of either AdCO or the AdCO moiety in AdCO-FL1 and a FL1 moiety are farther apart owing to the separately layered structure, rendering the efficiency of the energy transfer lower than that of *syn-1*. In addition, in the crystal of *anti-1*, there are more CO...HC interactions between the neighboring FL1 moieties than that in the crystal of *syn-1*. Thus, the softness of *anti-1* crystal structure is lower than that of *syn-1*. As a result, the intracrystalline CL reaction of *anti-1* is slower and the crystal of *anti-1* is more resistant to collapse of the crystalline state during the progress of the reaction.

Because the CL intensity corresponds to the amount of decomposition of the reactant per unit time, the duration of the CL emission and the magnitude of CL intensity indicate the continuity and rate of the reaction, respectively. Figure 9.12 shows the plot of CL intensities as a function of time for the reactions of *syn-1* and *anti-1* crystals heated to 140 and 160 °C, respectively. In contrast to the first-order reaction kinetics of the CL reaction of *syn-1* in solution, the crystalline-state kinetics data showed a nearly constant CL intensity for 10 min, followed by decay. In the case of *anti-1*, a gradual increase in the CL intensity was observed for 15 min, followed

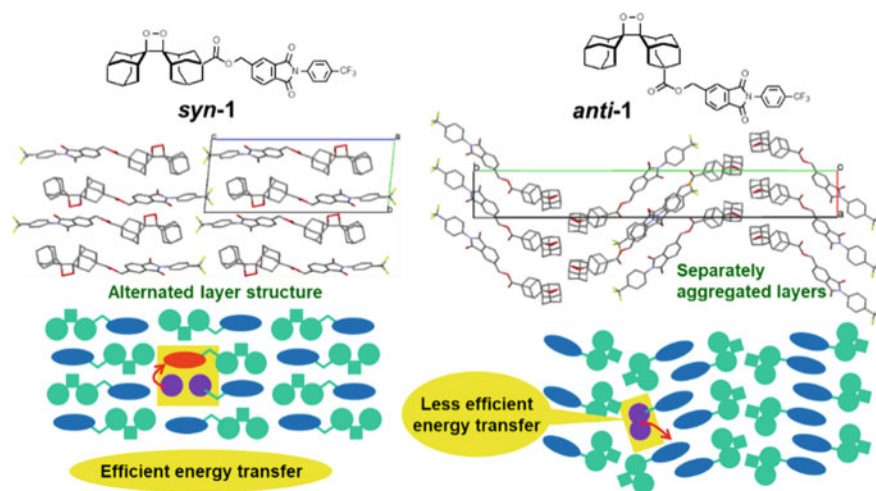
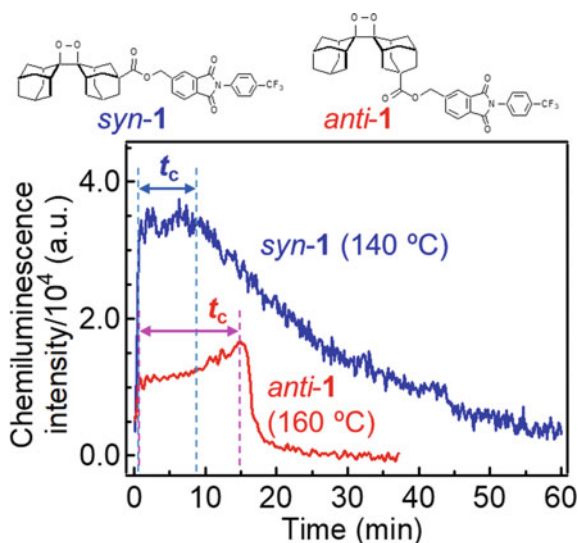


Fig. 9.11 Crystal structures of *syn-1* and *anti-1*

by rapid decay. In large crystals such as the LHP crystals, the CL reaction will begin from the heating surface where the crystal is in contact with the heater. Because the *syn-1* and *anti-1* crystals are in the size range of 1–300 μm , it is expected that the entire crystal will reach the desired temperature immediately after the heating has begun, resulting in instant CL reactions. However, a nearly constant CL intensity for *syn-1* and the gradual increase in the CL intensity for *anti-1* were observed during the time range t_c . These data indicate that the CL reaction exhibits zero-order kinetics, in which the reaction rate is independent of the concentration of the reactant; a constant number of the reactant molecules per unit time and per unit volume undergo the CL reaction (Fig. 9.13). The gradual increase in the CL intensity observed for *anti-1* suggests that in addition to exhibiting zero-order kinetics, the reaction is accelerated owing to the generated products. Therefore, the crystal structure of the reactant is maintained until the product accumulation reaches a certain threshold, beyond which a phase transition to the molten state occurs in both *syn-1* and *anti-1* (Fig. 9.14).

To confirm the zero-order kinetics of the CL reaction in crystals, it is necessary to analyze the reaction kinetics in a single crystal. Matsuhashi et al. investigated the CL reactions of a single crystal of Adox, which has a crystal size of 10–1000 μm [57]. When a single crystal of Adox was heated to 140 $^{\circ}\text{C}$, the CL intensity remained constant for 20 s to 10 min after the heating had begun and then decayed with time. Morphological observations of the heated crystals indicate that during the time interval of constant CL intensity, the crystalline state was maintained and the decay of the CL intensity correlated with the crystals being finely crushed. Because the values of the constant CL intensities are proportional to the volumes of the crystals used, it was concluded that the reaction rate depended on the number of molecules in the crystal. The constant CL intensity indicates that the CL reaction exhibits zero-order reaction kinetics.

Fig. 9.12 CL intensity as a function of time (min) for the reaction of *syn-1* crystals heated to 140 $^{\circ}\text{C}$ and *anti-1* crystals heated to 160 $^{\circ}\text{C}$



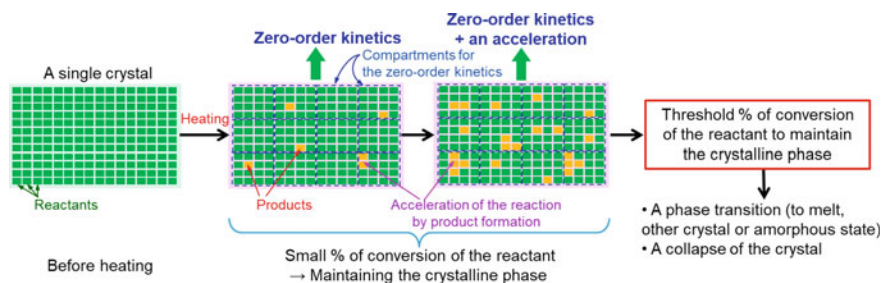


Fig. 9.13 Schematic diagram of the changes in a single crystal of the reactant during the course of a thermal reaction

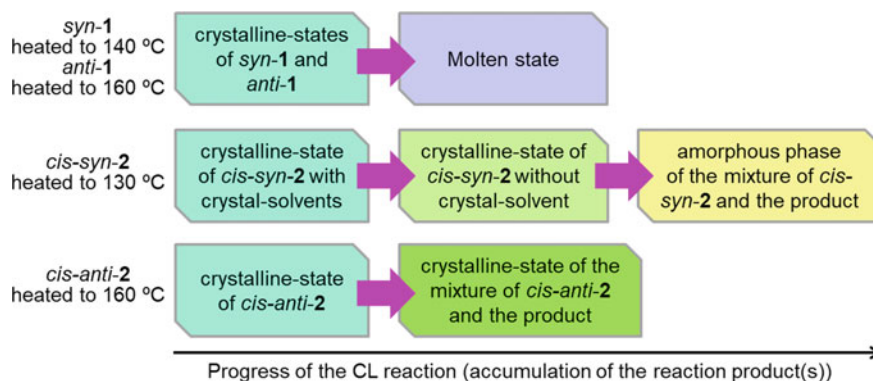


Fig. 9.14 Phase transitions induced by the accumulation of the products for the crystalline-state chemiluminescence reactions of *syn-1*, *anti-1*, *cis-syn-2*, and *cis-anti-2*

The Johnson–Mehl–Avrami–Kolmogorov (JMAK) model, which was proposed for the kinetics of crystalline phase transitions, was used to analyze the CL reaction in a single crystal of Adox. The zero-order reaction kinetics were confirmed by the analysis with the Sharp-Hancock equation for the JMAK model. After that, the first-order-like kinetics of the reaction were observed when the crystal was finely crushed. The CL reaction of Adox with a powder sample obtained by grinding bulk crystals also showed a first-order-like kinetic decay of the CL intensity, indicating that the reaction exhibits zero-order kinetics only with crystals of a certain size. The minimum compartment size of a reactant cluster in a crystal to exhibit zero-order kinetics will depend on the properties of the crystal (Fig. 9.13). Thermophysical measurements confirmed that a constant thermal diffusivity was maintained in the inside of a single Adox crystal during the zero-order reaction kinetics, indicating that the reaction field in the crystal was homogeneous and has become a thermal steady state. The accumulation of AdCO during the progress of the CL reaction causes crystal fracturing, which induces a change in the reaction kinetics.

The heated crystals of *syn-1* and *anti-1* showed a phase transition to the molten state induced by the accumulation of the products (Fig. 9.14). In the case of the di-substituted derivative **2**, which has two FL2 side chains, only one type of the product, AdCO-FL2 was produced by the CL reaction. Thus, the crystalline-state CL reactions of **2** were expected to show a change in the phase transition behavior. Solid-to-solid phase transitions were observed in the CL reactions of *cis-syn-2* and *cis-anti-2* in the crystalline state [56]. The crystals of *cis-syn-2* contain methylene chloride and *n*-hexane as crystalline solvents. When the crystals of *cis-syn-2* were heated to 130 °C, desorption of crystalline solvent molecules occurred during the first 15 min accompanied by a significant increase in the CL intensity. Thus, heating the crystals induced a transition from the crystalline phase containing crystalline solvents to the crystalline phase without the crystalline solvents (Fig. 9.14). Desorption of the crystalline solvents caused a change in the crystalline environment resulting in bent crystals and caused the acceleration of the CL reaction. In the subsequent 3 h, the accumulation of the product induced a transition from the crystalline phase without the crystalline solvents to the amorphous phase (Fig. 9.14) which correlated with a gradual increase in the CL intensity. The CL emission also showed a spectral change accompanied by these phase transitions, indicating that the molecular environment in the crystal was continuously changed by the phase transitions. The solvatochromic fluorescence property of the FL2 moiety in **2** and that of AdCO-FL2 were utilized to monitor the change in the intracrystalline environment. In contrast, the crystal of *cis-anti-2* heated to 160 °C maintained its crystal structure until 4 h of heating while the CL reaction progressed. The schematic diagram of the progress of the crystalline-to-crystalline phase transition from the phase of *cis-anti-2* to the phase of the mixture of *cis-anti-2* and AdCO-FL2 is shown in Fig. 9.14. During this phase transition, the intensity and the maximum wavelength of CL showed a characteristic change with time.

The relationship between the progress of an intracrystalline reaction and a phase transition has been first reported in the denitrogenation reaction of triazoline derivatives in crystals [58, 59], but more information is required to establish a general theory to explain the phase transition mechanisms. The data of phase transitions obtained by the crystalline-state CL reactions of **1** and **2** provide a basis for analyzing the relationship between the accumulation of the products and the lattice energy, as the accumulation of the products leads to the destruction of the crystal lattice. The relationships between the phase transitions and the kinetics of the CL reactions of *cis-syn-2* and *cis-anti-2* remain unclear. They are next challenging problems.

The CL reactions of Adox and its derivatives **1** and **2** proceed within a temperature range in which the crystalline states were maintained. Thus, they are soft crystal CL systems. However, if a crystal has a low melting point, its intracrystalline reactions cannot be studied by heating at a temperature above its melting point. Furthermore, a crystal lattice may reduce the reactivity of a CL substrate. For example, the thermolytic reaction of DPA endoperoxide (Fig. 9.7) does not proceed in the crystalline state when heated to 160 °C for 1 min, while its lifetime in solution is estimated to be only a few seconds at 160–200 °C. Interestingly, a crystal sample of DPA endoperoxide heated to 200 °C resulted in a singlet oxygen emission and the melting of

the crystal, indicating that the CL reaction proceeds with breaking the crystal lattice [60]. Thus, the crystal lattice structure has an important role to govern the reactivity by restricting the molecular motion for the reaction.

In this section, it was confirmed that the crystals of Adox and its derivatives **1** and **2** are soft crystals, which can undergo thermolytic reactions within the crystals. Hence, they are soft crystal CL systems, in which ongoing CL reactions can be tracked in real time by photon detection. The real-time analyses of their CL reactions provided valuable information on the intracrystalline reaction kinetics and the phase-transition inductions by the reaction progress, while there are still many unsolved problems described above. To establish the reaction theory to explain the relationships between crystal structures and reactivities, the energetics and kinetics of reactions, it is necessary to accumulate more data of intracrystalline reactions. For this purpose, the crystals of Adox and its derivatives **1** and **2** will be useful as role models to design novel soft crystal CL systems. Furthermore, it is expected that soft crystal CL systems exhibit molecular functions such as a stimulus-responsive property based on the unique CL reaction properties within the crystals. We expect further development of the chemistry of soft crystal CL systems learned from this text.

References

1. Garcia-Campana AM, Roman-Ceba M, Baeyens WRG (2001) Historical evolution of chemiluminescence. In: Garcia-Campana AM, Baeyens WRG (eds) *Chemiluminescence in Analytical Chemistry*. Marcel Dekker, New York, pp 1–39
2. Vacher M, Fdez Galv an I, Ding B-W, Schramm S, Berraud-Pache R, Naumov P, Ferre N, Liu Y-J, Navizet I, Roca-Sanjuan D, Baader WJ, Lindh R (2018) Chemi- and bioluminescence of cyclic peroxides. *Chem Rev* 118:6927–6974
3. Hirano T, Matsuhashi C (2022) A stable chemiluminophore, adamantylideneadamantane 1,2-dioxetane: from fundamental properties to utilities in mechanochemistry and soft crystal science. *J Photochem Photobiol C* 51:100483
4. Tanaka K, Toda F (2000) Solvent-free organic synthesis. *Chem Rev* 100:1025–1074
5. Kaupp G (2003) Solid-state molecular syntheses: complete reactions without auxiliaries based on a new solid-state mechanism. *CrystEngComm* 5:117–133
6. Kaupp G (2005) Organic solid state reactions with 100% yield. *Top Curr Chem* 254:95–183
7. James SL, Adams CJ, Bolm C, Braga D, Collier P, Friscic T, Grepioni F, Harris KDM, Hyett G, Jones W, Krebs A, Mack J, Maini L, Orpen AG, Parkin IP, Shearouse WC, Steed JW, Waddell DC (2012) Mechanochemistry: opportunities for new and cleaner synthesis. *Chem Soc Rev* 41:413–447
8. Wang GW (2013) Mechanochemical organic synthesis. *Chem Soc Rev* 42:7668–7700
9. Byrn SR, Xu W, Newman AW (2001) Chemical reactivity in solid-state pharmaceuticals: formulation implications. *Adv Drug Delivery Rev* 48:115–136
10. Glass BD, Novak C, Brown ME (2004) The thermal and photostability of solid pharmaceuticals - a review. *J Therm Anal Calorim* 77:1013–1036
11. Kato M, Ito H, Hasegawa M, Ishii K (2019) Soft crystals: flexible response systems with high structural order. *Chem Eur J* 25:5105–5112
12. Garcia-Campana AM, Baeyens WRG, Zhang X (2001) Chemiluminescence-based analysis: an introduction to principles, instrumentation, and applications. In: Garcia-Campana AM, Baeyens WRG (eds) *Chemiluminescence in Analytical Chemistry*. Marcel Dekker, New York, pp 41–65

13. McElroy WD, DeLuca M (1978) Chemistry of firefly luminescence. In: Herring PJ (ed) *Bioluminescence in Action*. Academic Press, London, pp 109–127
14. Shimomura O (2012) The fireflies and luminous insects, in *Bioluminescence: Chemical Principles and Methods*, rev. World Scientific Publishing, Singapore, pp 1–30
15. Contag CH, Bachmann MH (2002) Advances in in vivo bioluminescence imaging of gene expression. *Annu Rev Biomed Eng* 4:235–260
16. Greer III LF, Szalay AA (2002) Imaging of light emission from the expression of luciferases in living cells and organisms: a review. *Luminescence* 17:43–74
17. Iwano S, Sugiyama M, Hama H, Watakabe A, Hasegawa N, Kuchimaru T, Tanaka KZ, Takahashi M, Ishida Y, Hata J, Shimozono S, Namiki K, Fukano T, Kiyama M, Okano H, Kizaka-Kondoh S, McHugh TJ, Yamamori T, Hioki H, Maki S, Miyawaki A (2018) Single-cell bioluminescence imaging of deep tissue in freely moving animals. *Science* 359:935–939
18. Roda A, Guardigli M, Pasini P, Mirasoli M, Michelini E, Musiani M (2005) Bio- and chemiluminescence imaging in analytical chemistry. *Anal Chim Acta* 541:25–35
19. Yan Y, Shi P, Song W, Bi S (2019) Chemiluminescence and bioluminescence imaging for biosensing and therapy: in vitro and in vivo perspectives. *Theranostics* 9:4047–4065
20. Turro NJ, Lechtken P (1973) Thermal and photochemical generation of electronically excited organic molecules: tetramethyl-1,2-dioxetane and naphthvalene. *Pure Appl Chem* 33:363–388
21. Turro NJ, Lechtken P, Schore NE, Schuster G, Steinmetzer HC, Yekta A (1974) Tetramethyl-1,2-dioxetane. experiments in chemiexcitation, chemiluminescence, photochemistry, chemical dynamics, and spectroscopy. *Acc Chem Res* 7:97–105
22. Adam W (1982) Determination of chemiexcitation yields in the thermal generation of electronic excitation from 1,2-dioxetane. In: Adam W, Cilento G (ed), In *Chemical and Biological Generation of Excited States*. Academic Press, New York, pp. 115–152
23. Adam W, Beinhauer A, Hauer H (1989) Chapter 12 Activation parameters and excitation yields of 1,2-dioxetane chemiluminescence. In: Scaiano JC (ed) In *Handbook of Organic Photochemistry*, vol 2. CRC Press, Boca Raton, pp. 271–327
24. Ando Y, Niwa K, Yamada N, Enomoto T, Irie T, Kubota H, Ohmiya Y, Akiyama H (2008) Firefly bioluminescence quantum yield and color change by pH-sensitive green emission. *Nat Photonics* 2:44–47
25. Reguero M, Bernardi F, Bottoni A, Olivucci M, Robb MA (1991) Chemiluminescent decomposition of 1,2-dioxetanes: an MC-SCF/MP2 study with VB analysis. *J Am Chem Soc* 113:1566–1572
26. Vacher M, Farahani P, Valentini A, Frutos LM, Karlsson HO, Galvan IF, Lindh R (2017) How do methyl groups enhance the triplet chemiexcitation yield of dioxetane?". *J Phys Chem Lett* 8:3790–3794
27. Schuster GB (1979) Chemiluminescence of organic peroxides. Conversion of ground-state reactants to excited-state products by the chemically initiated electron-exchange luminescence mechanism. *Acc Chem Res* 12:366–373
28. Isobe H, Takano Y, Okumura M, Kuramitsu S, Yamaguchi K (2005) Mechanistic insights in charge-transfer-induced luminescence of 1,2-dioxetanones with a substituent of low oxidation potential. *J Am Chem Soc* 127:8667–8679
29. Wieringa JH, Strating J, Wynberg H, Adam W (1972) Adamantylideneadamantane peroxide: a stable 1,2-dioxetane. *Tetrahedron Lett.* 169–172
30. Schaap AP, Chen TS, Handley RS, DeSilva R, Giri BP (1987) Chemical and enzymatic triggering of 1,2-dioxetanes. 2. chemiluminescence from (tert-butyl(dimethylsilyl)oxy)-substituted dioxetanes. *Tetrahedron Lett* 28:1155–1158
31. McCapra F, Beheshti I, Burford A, Hann RA, Zaklika KA (1977) Singlet excited states from dioxetane *decomposition*. *J Chem Soc.* 944–946
32. Hummelen JC, Luider TM, Wynberg H (1987) Functionalized adamantylideneadamantane 1,2-dioxetanes: investigations on stable and inherently chemiluminescent compounds as a tool for clinical analysis. *Pure Appl Chem* 59:639–650
33. Schaap AP, Handley RS, Giri BP (1987) Chemical and enzymatic triggering of 1,2-dioxetanes. 1: Aryl esterase-catalyzed chemiluminescence from a naphthyl acetate-substituted dioxetane, *Tetrahedron Lett* 28:935–938

34. Hirano T (2016) Molecular origin of color variation in firefly (beetle) bioluminescence: a chemical basis for biological imaging. *Curr Top Med Chem* 16:2638–2647
35. Turro TJ, Ramamurthy V, Scaiano J (2010) Modern molecular photochemistry of organic molecules. University Science Books, Sausalito
36. Shimomura O (2012) The jellyfish *Aequorea* and other luminous coelenterates, in *Bioluminescence: Chemical Principles and Methods*, rev. Scientific Publishing, Singapore, pp 91–165
37. Koo JY, Schuster GB (1978) Chemiluminescence of diphenoyl peroxide-chemically-initiated electron exchange luminescence-new general mechanism for chemical production of electronically excited-states. *J Am Chem Soc* 100:4496–4503
38. Adam W, Kazakov DV, Kazakov VP (2005) Singlet-oxygen chemiluminescence in peroxide reactions. *Chem Rev* 105:3371–3387
39. Turro NJ, Chow MF, Rigaudy J (1981) Mechanism of thermolysis of endoperoxides of aromatic compounds: activation parameters, magnetic field, and magnetic isotope effects. *J Am Chem Soc* 103:7218–7224
40. Moureau C, Dufraise C, Butler CL (1926) Peroxyde de rubrene: nouvelles experiences. *Compt Rend Acad Sci* 183:101–105
41. Frankevich EL, Rummyantsev BM, Lesin VI (1975) Magnetic field effect on thermostimulated chemiluminescence of photoperoxidized rubrene. *J Lumin* 11:91–106
42. Höhne G, Schmidt AH, Lechtken P (1979) High energy molecules. part 4. Thermoanalysis of crystalline adamantylideneadamantone-1, 2-dioxetane. *Tetrahedron Lett.* 3587–3590
43. Lechtken P, Yekta A, Turro NJ (1973) Tetramethyl-1, 2-dioxetane: mechanism for an autocatalytic decomposition. Evidence for a quantum chain reaction. *J Am Chem Soc* 95:3027–3028
44. Turro NJ, Waddell WH (1975) Quantum chain processes: direct observation of high quantum yields in the direct and photosensitized excitation of tetramethyl-1,2-dioxetane. *Tetrahedron Lett.* 2069–2072
45. Kazakov VP, Voloshin AI, Ostakhov SS (1999) Quantum chain reactions with energetic branching: catalytic decomposition of dioxetanes. *Kinet Catal* 40:180–193
46. Roda A, Di Fusco M, Quintavalla A, Guardigli M, Mirasoli M, Lombardo M, Trombini C (2012) Dioxetane-doped silica nanoparticles as ultrasensitive reagentless thermochemiluminescent labels for bioanalytics. *Anal Chem* 84:9913–9919
47. Chen YJ, Mellot G, van Luijk D, Creton C, Sijbesma RP (2021) Mechanochemical tools for polymer materials. *Chem Soc Rev* 50:4100–4140
48. Yuan Y, Chen YI (2017) Visualized bond scission in mechanically activated polymers. *Chin J Polym Sci* 35:1315–1327
49. Chen Y, Spiering AJH, Karthikeyan S, Peters GWM, Meijer EW, Sijbesma RP (2012) Mechanically induced chemiluminescence from polymers incorporating a 1,2-dioxetane unit in the main chain. *Nat Chem* 4:559–562
50. Watanabe N, Takatsuka H, Ijuin HK, Wakatsuki A, Matsumoto M (2016) Hydrogen bonding network-assisted chemiluminescent thermal decomposition of 3-hydroxyphenyl-substituted dioxetanes in crystal. *Tetrahedron Lett* 57:2558–2562
51. Schramm S, Karothu DP, Lui NM, Commins P, Ahmed E, Catalano L, Li L, Weston J, Moriwaki T, Solntsev KM, Naumov P (2019) Thermochemiluminescent peroxide crystals. *Nat Commun* 10:1–8
52. Matsumoto M (2004) Advanced chemistry of dioxetane-based chemiluminescent substrates originating from bioluminescence. *J Photochem Photobiol C* 5:27–53
53. White EH, Harding MJC (1965) Chemiluminescence in liquid solutions. Chemiluminescence of lophine and its derivatives. *Photochem. Photobiol* 4:1129–1155
54. Boaro A, Reis RA, Silva CS, Melo DU, Pinto AGGC, Bartoloni FH (2021) Evidence for the formation of 1,2-dioxetane as a high-energy intermediate and possible chemiexcitation pathways in the chemiluminescence of lophine peroxides. *J Org Chem* 86:6633–6647
55. Matsuhashi C, Ueno T, Uekusa H, Sato-Tomita A, Ichiyanagi K, Maki S, Hirano T (2020) Isomeric difference in the crystalline-state chemiluminescence property of an adamantylideneadamantane 1,2-dioxetane with a phthalimide chromophore. *Chem Commun* 56:3369–3372

56. Matsuhashi C, Oyama H, Uekusa H, Sato-Tomita A, Ichiyanagi K, Maki S, Hirano T (2022) Crystalline-state chemiluminescence reactions of two-fluorophore-linked adamantylideneadamantane 1,2-dioxetane isomers accompanied by solid-to-solid phase transitions. *CrystEngComm* 24:3332–3337
57. Matsuhashi C, Fujisawa H, Ryu M, Tsujii T, Morikawa J, Oyama H, Uekusa H, Maki S, Hirano T (2022) Intracrystalline kinetics analyzed by real-time monitoring of 1,2-dioxetane chemiluminescence reaction in a single crystal. *Bull Chem Soc Jpn* 95:413–420
58. de Loera D, Garcia-Garibay MA (2012) Efficient aziridine synthesis in metastable crystalline phases by photoinduced denitrogenation of crystalline triazolines. *Org Lett* 14:3874–3877
59. de Loera D, Stopin A, Garcia-Garibay MA (2013) Photoinduced and thermal denitrogenation of bulky triazoline crystals: Insights into solid-to-solid transformation. *J Am Chem Soc* 135:6626–6632
60. Yamasaki N, Matsuhashi C, Maki S, Hirano T (2021) Singlet-oxygen chemiluminescence from heated crystal samples of 9,10-diphenylanthracene endoperoxides. *Chem Lett* 50:1681–1683

Open Access This chapter is licensed under the terms of the Creative Commons Attribution 4.0 International License (<http://creativecommons.org/licenses/by/4.0/>), which permits use, sharing, adaptation, distribution and reproduction in any medium or format, as long as you give appropriate credit to the original author(s) and the source, provide a link to the Creative Commons license and indicate if changes were made.

The images or other third party material in this chapter are included in the chapter's Creative Commons license, unless indicated otherwise in a credit line to the material. If material is not included in the chapter's Creative Commons license and your intended use is not permitted by statutory regulation or exceeds the permitted use, you will need to obtain permission directly from the copyright holder.

